is greater for the methylated derivative. Our analysis indicates that any low-symmetry distortion is much smaller than for the d^4 metallocenes.

Acknowledgment. We thank the United Kingdom Science and Engineering Research Council and the Royal Society for their support of this work.

Registry No. Cp_2Mo, 51370-80-0; Cp_2W, 51481-44-8; Cp_2Re, 56261-86-0; Cp_2*Re, 98814-97-2; $(tol)_2V$, 12131-27-0.

Stacked Complexes of Iridium and a Novel Form of Charge Compensation

Paul G. Rasmussen,* J. Bruce Kolowich, and Juan Carlos Bayón†

Contribution from the Department of Chemistry, University of Michigan, Ann Arbor, Michigan 48109. *Received November 18, 1987*

Abstract: Mixed valence metal chain compounds based on the monoanion $[Ir(CO)_2Tcbiim]^-$ were investigated (Tcbiim = 4,4',5,5'-tetracyano-2,2'-biimidazole, a dianion). These compounds were prepared by inert atmosphere electrochemical oxidation with a variety of alkyl ammonium cation based electrolytes. Synthetic details are presented for the preparation of several asymmetric alkyl ammonium cations, and the subsequent electrolyte salt preparation. The technique for electrochemical oxidation is described in detail. Single-crystal X-ray solutions are presented for three complex Ir(I) salts: $NEt_3Me[Ir(CO)_2Tcbiim]\cdot{}^1/_2CH_3CN$, $NEt_2Me_2[Ir(CO)_2Tcbiim]$, and a dication salt $NEt_2Me(CH_2)_4NEt_2Me[Ir(CO)_2Tcbiim]_2$. The first of these crystallizes in the space group *Pnnm* with $a = 6.918$ Å, $b = 22.223$ Å, $c = 15.101$ Å, and $Z = 4$. A final agreement of $R = 4.25\%$ for 133 parameters with 972 retained data was obtained. The second crystallized in the space group $P2_12_12$ with $a = 7.074$ Å, $b = 19.698$ Å, $c = 15.336$ Å, and $Z = 4$. The obtained final agreement was $R = 3.94\%$ for 236 parameters with 1505 retained data. The dication structure was refined in the nonstandard space group $P22_12_1$ with $a = 15.751$ Å, $b = 7.233$ Å, $c = 19.135$ Å, and $Z = 4$. A final agreement of $R = 5.1\%$ for 130 parameters with 789 retained data was found. Solid-state packing for this series of compounds is discussed. Packing diagrams reveal molecular interactions responsible for earlier observations of thermochromic behavior. A series of insoluble mixed valence compounds formulated as $[cat]_5[Ir(CO)_2Tcbiim]_6[an]$ where [cat][an] denotes included supporting electrolyte were prepared. Conductivity data are presented. A reaction of $[cat]_4[Ir(CO)_2Tcbiim]_6$ with an isoelectronic analogue of the stacking unit $[Pt(CN)_2Tcbiim]^{2-}$ produced a unique one-dimensional alloy in single-crystal form. This compound, $[NEt_3Me]_3[Ir(CO)_2Tcbiim]_2[Pt(CN)_2Tcbiim]\cdot 3CH_3CN$, crystallized in the space group $P2_1$ with $a = 13.412$ Å, $b = 6.874$ Å $c = 13.409$ Å, and $\beta = 111.21°$. Here, $Z = 2$, however; since there is one metal atom in the asymmetric unit, the stacking units are disordered along the stack. Perspective plots clearly reveal a metal atom chain. Final agreement of $R = 4.01\%$ was observed for 223 parameters with 2227 retained data.

In the realm of class III mixed-valence compounds, there are relatively few that have been synthesized by conscious design, and none that we are aware of wherein a hetero bimetallic system yields a crystallographically identical site for two metals in different oxidation states. We report here on the synthesis and characterization of such a system based on complexes of tetracyanobiimidazole. Some of the coordinating tendencies of this ligand have been previously reviewed.[1]

The starting point for this system is the planar anion $[Ir(CO)_2Tcbiim]^-$ where $H_2Tcbiim$ is 4,4',5,5'-tetracyano-2,2'-biimidazole, an acidic molecular comparable to oxalic acid. This planar ion associates weakly in solution and precipitates as a brightly colored solid. The color of the solid varies with the counter cation. Under electrolytic oxidation this ion associates strongly and forms a linear-chain mixed-valence semiconductor that grows on the anode. This material has an unusual charge compensation mode. Partial oxidation of the iridium apparently leads to disorder on the counter cation site. To solve this problem we introduce the isoelectronic ion $[Pt(CN)_2Tcbiim]^{2-}$ into the solution. The structure and properties of the pure linear chain and the novel one-dimensional alloy are described below.

The isolation of single crystals of iridium chain compounds has proven difficult, although classic work by Ginsberg et al.[2] and Reis[3] showed that it could be done. The isoelectronic substitution method we describe may prove generally useful in aiding crystallization in partially oxidized systems.

Experimental Section

Physical Measurements. Elemental analyses were performed by Spang Microanalytical Laboratory, Eagle Harbor, MI 49951, or Galbraith Laboratories Inc., Knoxville, TN 37921.

Infrared spectra (4000–200 cm^{-1}) of samples confined as KBr pellets, or as Nujol mulls placed between NaCl, KBr, or AgCl plates, were recorded on a Perkin-Elmer Model 1330 grating spectrophotometer.

Proton NMR spectra were recorded on a Brucker WM-360. All proton resonances are reported relative to TMS, except those recorded in D_2O, which are reported relative to DSS.

Two contact pellet conductivities were measured with a simple press. The base of the press was constructed from a solid block of aluminum and the barrel and plunger are composed of steel. The plunger is insulated from the barrel with a nylon sleeve, and conductivity is measured from the plunger to the base while pressure is applied.

Scanning electron microscope work was performed on a Hitachi Model S-570. The geology department of the University of Michigan acknowledges support from NSF Grant No. BSR-83-14092 for the purchase of this new microscope in 1985.

Electron microprobe analysis was performed on a Cameca-MBX, purchased for the University geology department with support from NSF Grant No. BAR-82-12764 in 1984.

Powder diffraction patterns were recorded on a North American Phillips Co. type 52056-8 Debye-Sherrer camera, mounted on a Phillips X-ray source equipped with a Copper Kα X-ray tube.

† Present address: Universitat Autõnoma de Barcelona, Bellaterra, 08193 Barcelona, Spain

(1) Avery, J., Dahl, J. P., Ed. *Understanding Molecular Properties*; D. Reidel: Hollard, 1987; pp 187–194.
(2) Ginsberg, A. P.; Koepke, J. W.; Hauser, J. J.; West, K. W.; DiSalvo, F. J.; Sprinkle, C. R.; Cohen, R. L. *Inorg. Chem.* **1976**, *15*, 514.
(3) Reis, A. H.; Peterson, S. W. *Ann. N.Y. Acad. Sci.* **1978**, *313*, 560.

0002-7863/88/1510-7042$01.50/0

Table I. Soluble Salts of $[Ir(CO)_2Tcbiim]^-$. Electrolytic Oxidation Results

cation	electrolyte anion	result
$NPrEt_2Me^+$	BF_4^-	conducting solid
NEt_3Me^+	BF_4^-	conducting solid
NEt_3Me^+	HSO_4^-	conducting microcrystals
NEt_3Me^+	FSO_3^-	conducting solid
$NEt_2Me_2^+$	BF_4^-	conducting solid
$NEt_2Me_2^+$	HSO_4^-	conducting solid
$NEt_2Me_2^+$	$PO_2(OMe)_2^-$	dark solution
$C(NH_2)_3^+$	NO_3^-	dark solution
$C(NH_2)_3^+$	ClO_4^-	dark solution
Na^+	ClO_4^-	dark solution
Na^+	none	dark solution

Table II. Less Soluble or Insoluble Salts of $[Ir(CO)_2Tcbiim]^-$. Electrolytic Oxidation Results

cation	electrolyte anion	result
$NPrEt_3^+$	BF_4^-	metastable solid
NEt_4^+	BF_4^-	conducting microcrystals
NEt_4^+	ClO_4^-	conducting solid
NEt_4^+	HSO_4^-	conducting microcrystals
NEt_4^+	none	dark solution
$(NEt_2MeCH_2CH_2)_2^{2+}$	$PO_2(OMe)_2^-$	red and blue crystals
$(NEt_2MeCH_2CH_2)_2^{2+}$	HSO_4^-	conducting solid
$NEtMe_3^+$	BF_4^-	poor conductor
NMe_4^+	BF_4^-	light solution

Dielectric constant measurements were performed immersed in a dewer using a parallel plate device equipped with platinum resistance thermometers and a General Radio type 1605-A impedance comparator as described by Gentry.[4]

Synthesis. Synthesis of Tetracyanobiimidazole ($H_2Tcbiim$)[5] and $Na[Ir(CO)_2Tcbiim]$[6] has been previously reported.

Synthesis of $C(NH_2)_3[Ir(CO)_2Tcbiim]$. A suspension of $(C(NH_2)_3)_2Tcbiim$ and $[Ir(COD)Cl]_2$ was stirred in refluxing CH_3CN for several hours. After cooling to room temperature, byproduct $C(NH_2)_3Cl$ was removed by filtration, and the volume was reduced under vacuum to about 10 mL. The remaining orange solution was allowed to stand in the refrigerator overnight, resulting in the formation of yellow-orange crystals. These were removed via filtration and redissolved in 15 mL of fresh CH_3CN. Introduction of carbon monoxide produced a dramatic color change, and the gas was bubbled through the solution for 1 h. The volume of the resulting dark blue-black solution was reduced under vacuum, and the solution was left to stand in the refrigerator overnight. The blue product was filtered off. This product is best stored under dry nitrogen.

Average yield ~60%.

Synthesis of $(NH_4)_2[Pt(CN)_2Tcbiim]$. Anhydrous $Pt(CN)_2$ must first be prepared from $(NH_4)_2Pt(CN)_4$ by very careful heating of the solid at 300 °C in air for ca. 20 min.[7] Caution must be observed as byproduct gases include HCN and NH_3. The $Pt(CN)_2$ obtained is stirred in (concentrated) NH_4OH for several minutes and the liquid pulled off in vacuo. The residue is neutral *cis*-$Pt(NH_3)_2(CN)_2$. This product is stirred with $H_2Tcbiim$ in refluxing CH_3CN for several hours. The $(NH_4)_2[Pt(CN)_2Tcbiim]$ precipitates after volume reduction and cooling at 0 °C overnight. The product can be recrystallized as white needles from CH_3CN. Overall yield 20%.

A sample of $(NBu_4)_2[Pt(CN)_2Tcbiim]$ was prepared by dissolving $(NH_4)_2[Pt(CN)_2Tcbiim]$ in CH_3CN and precipitating the desired compound with NBu_4OH. The precipitated solid was recovered by filtration, and residual NH_4OH and NBu_4OH were removed by evacuation. The solid was recrystallized from CH_3CN/ether to give pure, white $(NBu_4)_2[Pt(CN)_2Tcbiim]$.

Cations. The mixed alkyl ammonium iodides used as cation sources for the organometallic salts shown in Tables I and II are not available commercially but are readily prepared by reaction of the appropriate amine with an alkyl iodide. The following procedure is typical. A solution of 0.02 mol of the amine in 50 mL of diethyl ether is stirred while 0.02 mol of the alkyl iodide is added. The mixture is held at reflux for a period of several hours to several days. Higher alkyl iodides require longer reaction times. The solution is cooled, and the white precipitate is removed by filtration. The typical yield of quaternary ammonium iodide is about 85%. Proton NMR data for the synthesized cations has been recorded.[8]

Electrolyte Salts. Electrolyte salts were prepared in anhydrous form by a variety of methods. Generally, preparation involved a precipitation using an alkyl ammonium iodide or titration of an alkyl ammonium hydroxide. The product salts were purified by recrystallization from dry organic solvents.[9]

Alkyl Ammonium Salts of $[Ir(CO)_2Tcbiim]^-$. Two methods were employed in the preparation of these salts, the choice depending on the subsequent reaction. Both involve the reaction of $Na[Ir(CO)_2Tcbiim]$ with one of the synthesized alkyl ammonium salts. The second method is more tedious, but it is designed to produce much purer compounds.

Direct Precipitation of $[Ir(CO)_2Tcbiim]^-$. These salts are usually prepared with the intent of use in a subsequent electrochemical reaction. The common solvent for these subsequent electrolytic oxidations is CH_3CN. In these reactions, the prior synthesized alkyl ammonium salts are used in the formation of background electrolyte solutions. $Na[Ir(CO)_2Tcbiim]$ is a soluble form of $[Ir(CO)_2Tcbiim]^-$, and it reaches saturation at ~0.04M. With CH_3CN as solvent, addition of a concentrated solution of an alkyl ammonium electrolyte salt ($NR_4(an)$) to a saturated solution of $Na[Ir(CO)_2Tcbiim]$ will result in precipitation of $NR_4[Ir(CO)_2Tcbiim]$. Separation of this compound from the mixture by filtration is possible if Na(an) is soluble in CH_3CN.

Nitrate Method for Preparation of Alkyl Ammonium Salts of $[Ir(CO)_2Tcbiim]^-$. The success of this method relies on the fact that sodium nitrate is virtually insoluble in CH_3CN. The reaction involves mixing a dilute solution of $Na[Ir(CO)_2Tcbiim]$ with a stoichiometric equivalent of an alkyl ammonium nitrate, also dissolved in CH_3CN. This mixing is best accomplished by slow stirring of one component, while the other is added dropwise.

Sodium nitrate begins to precipitate immediately and is removed from solution by filtration on completing the addition. The volume of the remaining yellow solution is reduced to ~10 mL and the solution cooled in the refrigerator overnight. The product salts are easily recovered by filtration.

Average yield ~85%.

Alkyl Ammonium Dications. In an attempt to promote crystal growth through interstack binding, a dication was synthesized. This was essentially two alkyl ammonium cations bound together by an aliphatic bridge. A salt of this dication with $[Ir(CO)_2Tcbiim]^-$ was crystallized and the X-ray structural solution completed. The compound packs in a manner most analogous to the previously reported salt $NEt_4[Ir(CO)_2Tcbiim]$,[10] except that the dications are associated with two distinct anion stacks. Attempts at electrochemical oxidation were hampered by the extremely low solubility of this compound. Currents were lowered to the nanoamp range to compensate for this low solubility, but the conducting solids obtained possessed no greater crystallinity than other cation forms.

Mixed-Valence Compounds of Iridium. These compounds are electrochemical oxidaaion products of $[Ir(CO)_2Tcbiim]^-$. While numerous compounds were produced, the assembly and setup of the reaction differs with the solubility of the starting material. A special three-compartment electrochemical cell and specific platinum electrodes were designed and constructed for these reactions.

Synthesis of $(cat)_5[Ir(CO)_2Tcbiim]_6(an)$ from Soluble $(cat)[Ir(CO)_2Tcbiim]$. In this context, soluble means any starting material that will completely dissolve in the anode compartment before a reaction is begun. Practically, this means that 30–40 mg of the starting material (the common amount) must dissolve in 10 mL of electrolyte (anode volume). For $(cat)[Ir(CO)_2Tcbiim]$, this is true for cat = Na^+, $C(NH_2)_3^+$, $NPrEt_2Me^+$, NEt_3Me^+, and $NEt_2Me_2^+$. These compounds are soluble enough to use the following method.

Cell and Electrode Preparation. The cell cleaning required several days. The cell was rinsed and filled with fuming nitric acid (caution). After the cell was soaked for a day or two, the acid was removed and the cell rinsed thoroughly with water. After the cell was soaked for several days in water, the rinse and soak procedure was repeated with CH_3CN. (Since guanidinium nitrate is insoluble in CH_3CN, when it was used, acetone was substituted as the reaction solvent.) The CH_3CN was removed and the cell pumped dry and refilled with fresh, high-purity CH_3CN.

The electrodes were cleaned by soaking in fuming nitric acid for 15–20 min. They were rinsed with water and conditioned by potential cycling

(4) Gentry, A. Ph.D. Thesis, University of Michigan, 1983, p 27.
(5) Rasmussen, P. G.; Hough, R. L.; Anderson, J. E.; Bailey, O. H.; Bayoñ, J. C. *J. Am. Chem. Soc.* **1982**, *104*, 6155.
(6) Bailey, O. H. Ph.D. Thesis, The University of Michigan, 1983, p 39.
(7) Baranovskii, B.; Kharitonov, Y. Y. *Dokl. Akad. Nauk SSSR* **1966**, *169* (6), 1335.
(8) Kolowich, J. B. Ph.D. Thesis, The University of Michigan, 1987, p 24.
(9) Kolowich, J. B. Ph.D. Thesis, The University of Michigan, 1987, p 25.
(10) Rasmussen, P. G.; Bailey, O. H.; Bayoñ, J. C.; Butler, W. M. *Inorg. Chem.* **1985**, *23*, 343.

at ~4 V, changing polarity every 10 s for 3 or 4 min. The final cycle was ended with the anode (in the future reaction) functioning as a cathode (in the cycling apparatus). This ensured a "hydrogen protected" surface on the anode. These electrodes were carefully rinsed with water and then CH_3CN and placed in the cell, still filled with clean CH_3CN.

Cell Assembly. The CH_3CN was removed from the clean cell and it was dried by evacuation. The starting material was weighed and placed in a clean 50 mL Schlenk flask. An 0.1 M solution of the appropriate electrolyte was prepared. The starting material was then dissolved in 10 mL of the electrolyte solution, and the resulting dark solution was warmed slightly and filtered. The cathode and center compartments of the cell were filled with electrolyte and the filtered starting material solution was transferred into the anode compartment. Care must be taken to ensure that the levels are the same in all compartments. The filled cell was placed in a constant temperature environment and connected to a DC power source. The sources used for these reactions were of two varieties. A constant current source was used in crystallization attempts, and a constant potential source was employed if information on changes in cell resistance was desired.

Typically, the current was adjusted to a value in the microamp range and left for several days or weeks untouched. If the product was an insoluble conducting solid, it slowly precipitated on the anode during this time. It was recovered by disconnecting the power supply and carefully removing the anode from the cell. The product was removed from the electrode by scraping it off with a dull knife.

Synthesis of (cat)$_5$[Ir(CO)$_2$Tcbiim]$_6$(an) from Less Soluble or Insoluble (cat)[Ir(CO)$_2$Tcbiim]. In this case, less soluble means any starting material that will not dissolve completely in the available electrolyte in the anode. Compounds of this type are of the form (cat)[Ir(CO)$_2$Tcbiim] where cat = $NPrEt_3^+$, NEt_4^+, $NEtMe_3^+$, NMe_4^+, and $(NEt_2MeCH_2CH_2)_2^{2+}$. Electrochemical oxidations were performed in a manner similar to that of the soluble compounds, with the only difference being the method of starting material introduction. Since the starting material is relatively insoluble, it cannot be dissolved and filtered. Instead, the weighed sample was placed in the dry anode compartment, and dryness was ensured by holding the cell in vacuo for 1 h at 50 °C. Supporting electrolyte was then transferred to all three cell compartments.

The results of these oxidations are summarized in Tables I and II. The designation "conducting solid" in the table indicates that partially oxidized material deposits on the anode.

Reaction of Mixed-Valence Iridium Compound with Isoelectronic Platinum Analogue. Although numerous mixed-valence compounds of iridium were synthesized, none could be prepared in a crystalline form suitable for single-crystal X-ray analysis. If the mixed-valence compound is prepared as (cat)$_4$[Ir(CO)$_2$Tcbiim]$_6$ (soluble, cation deficient) then only an amorphous form could be obtained. When electrolyte is present, the conducting solid deposits as (cat)$_5$[Ir(CO)$_2$Tcbiim]$_6$(an). In this case the extra mole of salt should fill the empty sites and add binding energy, and although the degree of crystallinity actually did increase and powder patterns were obtained for many solid compounds, the cations and anions are probably disordered on a common site.

A second method for affecting charge compensation in the stack is by substituting an isoelectronic analogue, with a different net negative charge. The anion [Pt(CN)$_2$Tcbiim]$^{2-}$ was available. Substitution of a portion of [Ir(CO)$_2$Tcbiim]$^-$ with this platinum analogue could allow the metal stack to have an average charge of 1- per stacking unit, filling all the cation sites.

A sample of $(C(NH_2)_3)_4$[Ir(CO)$_2$Tcbiim]$_6$ was prepared by electrochemical oxidation and precipitated by the method described above. A solution of 32 mg of this compound in 50 mL of CH_3CN was prepared, and a solution of 20 mg of $(NBu_4)_2$[Pt(CN)$_2$Tcbiim] in 50 mL of CH_3CN was added slowly over the course of 48 h. When the expected precipitation did not occur, 30 mL of toluene was added to the mixture and the volume was reduced through the fast port of the vacuum line to 35 mL. A black solid preicpitated during this volume reduction and was recovered by filtration. This solid was redissolved in 10 mL of CH_3CN and precipitated by addition of 4 mL of a concentrated CH_3CN solution (~150 mg/k mL) of triethylmethylammonium nitrate. The precipitated solid was again recovered by filtration, and the dark solid (~20 mg) was redissolved in 1 mL of warm CH_3CN. The resulting warm yellow solution was transferred to a freshly reblown 5-mL round-bottom flask and placed in a thick walled insulating styrofoam container to cool slowly for 48 h. Crystals formed as optically dichroic plates, appearing green in cross section, deep red along the longest sides, and very dark along the short edges. These crystals desolvated immediately upon exposure to any non-CH_3CN saturated atmosphere to yield small, very dark pieces.

Analysis of individual crystals by electron microprobe yielded an iridium/platinum ratio of 2/1. If the iridium oxidation state was 1.33 and the platinum(II), the expectation was that this ratio would be 3/1. The likely range in the value was ±0.25 of a unit. This value could be accommodated by having formally Ir(I), Ir(II), and Pt(II) in equal proportions along the stack; however, the question of whether the oxidation state is best described as 2 × Ir(1.5) + Pt(II) or as 2 × Ir(1.33) + Pt(2.33) is difficult to answer. The excellent crystal structure solution quality and lack of evidence of disorder along the metal atom chain support the latter representation.

Crystal Growth and Crystallography. (1) NEt$_3$[Ir(CO)$_2$Tcbiim]. Single crystals of this compound were prepared by thermal recrystallization from CH_3CN. Twenty milligrams of the compound were dissolved in a minimum volume of solvent (~3 mL). The resulting red solution was placed in an insulating styrofoam container and this container then placed in a refrigerator at 0 °C for several days. During this period, several long yellow needles formed free in the solution. When exposed to air, these needles turned dark red within 60–70 s. This color change was believed to be a result of desolvation, since the red needles could be redissolved in CH_3CN and reprecipitated as yellow needles. Isolation of the yellow form of the compound was accomplished by cautions gravity filtration in a solvent-saturated atmosphere. One fairly large crystal was shortened to 2 mm and quickly transferred to a 0.3-mm X-ray capillary.

(2) NEt$_2$Me$_2$[Ir(CO)$_2$Tcbiim]. This compound can be recrystallized thermally from CH_3CN as dark red needles. However, better crystals were obtained by slow "salting out" of the compound from CH_3CN with $NEt_2Me_2NO_3$. The details of this procedure are described elsewhere.[11]

(3) Et$_2$MeN(CH$_2$)$_4$NMeEt$_2$[Ir(CO)$_2$Tcbiim]$_2$. This compound was crystallized by a similar "salting out" process with $Et_2MeN(CH_2)_4NMeEt_2[PO_2(OMe)_2]_2$ in CH_3CN. The red prisms displayed no evidence of air sensitivity or desolvation, but they were nevertheless sealed in a 0.3-mm capillary for data collection.

(4) (NEt$_3$Me)$_3$[Ir(CO)$_2$Tcbiim]$_2$[Pt(CN)$_2$Tcbiim]. Single crystals of this compound were prepared by thermal recrystallization from CH_3CN. The specific method used is described in the Experimental Section. One crystal was covered with purified hydrocarbon grease while still in the mother liquor and then quickly transferred to and sealed in an 0.3-mm X-ray capillary.

Data Collection and Program Description. The method of data collection did not appreciably vary from sample to sample. Each crystal was mounted on a goniometer head and placed in position on a Syntex P$\bar{1}$ four-circle diffractometer. Preliminary photographs with $2\theta = 0$ were taken, and the reflections obtained were used to calculate possible cell axes and angles. From these values unit cell parameters were determined, and axial photographs of zero levels were obtained. A centering program was executed to obtain least-squares values for cell parameters and their errors. Intensity data were collected by scanning θ at a rate based on reflection intensity, after an orientation matrix had been calculated. Background intensity was measured on every scan. The time period for background collection was based on a consistent fraction of the neighboring counting intensity.

Three standard reflections were selected and monitored for crystal decay or movement. These reflections were measured after every 50 reflections; change of 3–4% was considered normal, 10% grounds for discontinuing data collection.

Solution refinement was completed using the SHELX program package by Sheldrick.[12] Initial solution was most frequently accomplished with the direct methods program MULTAN.[13] Least-squares refinement was performed with ORFLS,[14] which minimizes the factor

$$\sum w(|F_o| - |F_c|)^2$$

Here F_o is the observed structure factor for a given reflection, and F_c is the calculated structure factor. The distances between atoms and their bond angles were calculated by using the program ORFEE,[15] and HFINDR[16] enabled idealized hydrogen atom positions to be calculated. Atomic scattering factors and correction terms were obtained from The *Inter-*

(11) Kolowich, J. B. Ph.D. Thesis, The University of Michigan, 1987, p 56.

(12) Sheldrick, G., The "SHELX" program package; Institute für Anorganische Chemie der Universität Göttingen (FRD); 1978.

(13) Main, P.; Woolfsen, N. M.; Germain, G. MULTAN, Direct Methods Program; University of York (UK); 1978.

(14) Bushing, W. R.; Martin, K. O.; Levy, H. A. ORFLS—A Fortran Crystallographic Least Squares Program; Oak Ridge National Laboratory; 1962.

(15) Bushing, W. R.; Martin, K. O.; Levy, H. A. ORFFE—A Fortran Crystallographic Function and Error Program; Oak Ridge National Laboratory.

(16) Zalkin, A. *A Program to Calculate Hydrogen Positions*; Lawrence Berkeley Laboratory; 1973; modified by D. Ward; Lawrence Berkeley Laboratory; 1974.

national Tables for X-ray Crystallography,[17] and the published table of Cromer and Waber.[18]

After refining the solution to convergence, the program STD-DEV[19] allowed for calculation of standard deviations of atomic coordinates and thermal parameters. Calculation of least-squares planes was accomplished with GEOMIN.[20] Molecular drawings were performed with the program ORTEP;[21] however, the majority of the drawings presented are packing plots. These were prepared with PLUTO.[22]

Agreement factors used to test the validity of the proposed structure are

$$R = \frac{\sum(|F_o| - |F_c|)}{\sum|F_o|}$$

and

$$R_w = \left(\frac{\sum w(|F_o| - |F_c|)^2}{\sum wF_o^2}\right)^{1/2}$$

Solution and Refinement. (1) $NEt_3Me[Ir(CO)_2Tcbiim]$. Axial photographs indicated the symmetry of an orthorhombic space group. Examination of the collected data gave rise to observed extinctions: $h00$, $h = 2n + 1$; $0k0$, $k = 2n + 1$; $00l$, $k = 2n + 1$; $h0l$, $h + l = 2n + 1$; $0kl$, $k + 1 = 2n + 1$. These absences correspond to the symmetry of the Laue group *mmm*, space group *Pnnm* (No. 58). A summary of the data collection and crystallographic parameters appears in Table 1.S. The final convergence gave $R = 4.25\%$ and $R_w = 3.78\%$ with 972 retained data. The final data to parameter ratio was 7.3:1. In the final difference Fourier map, no peak greater than 0.74 eÅ^{-3} could be located. Final positional and thermal parameters are collected in Tables 2.S and 3.S. The asymmetric unit and its connected mirror image are shown in Figure 1.S.

(2) $NEt_2Me_2[Ir(CO)_2Tcbiim]$. Axial photographs indicated the symmetry of an orthorhombic space group. Examination of the collected data gave rise to the following observed extinctions: $h00$, $h = 2n + 1$; $0k0$, $k = 2n + 1$. These correspond to the symmetry of the Laue group 222, space group $P2_12_12$ (No. 18). Table 4.S contains a summary of the data collection and crystallographic parameters.

After all atoms were located and refined, an absorption correction was applied, and anisotropic thermal parameters were calculated for the ligand atoms. Several cycles of refinement led to convergence with $R = 3.94\%$ and $R_w = 3.94\%$. In the final difference map, the largest residual seen corresponded to 0.94 eÅ^{-3}, located directly between the closest approach of the metal atoms. In the final refinement, 1505 data were retained. Since 236 parameters were used, the final data to parameter ratio was 6.38:1. This value is low, and no further anisotropic parameters were calculated. Final positional and thermal parameters appear in Tables 5.S and 6.S, and the asymmetric unit is shown in Figure 2.S.

(3) $Et_2MeN(CH_2)_4NMeEt_2[Ir(CO)_2Tcbiim]_2$. Axial photographs again indicated the presence of an orthorhombic space group. Examination of the collected data produced the following observed extinctions: $0k0$, $k = 2n + 1$; $00l$, $l = 2n + 1$. These correspond to the symmetry of the Laue group 222, space group $P22_12_1$. The corresponding standard group is No. 18, $P2_12_12$. Crystallographic parameters are collected in Table 7.S. A solution was obtained for this data set with the program MULTAN. Final convergence was obtained with $R = 5.1\%$ and $R_w = 3.7\%$. Since 789 data were retained, the variable to data ratio was 6.0:1. Due to this low value, only the central metal received anisotropic thermal parameters. The largest residual in the final difference map was 1.08 Å^{-3} and was located in the cation region. Final positional and thermal parameters are collected in Tables 8.S and 9.S, and the asymmetric unit is shown in Figure 3.S.

(4) $(NEt_3Me)_3[Ir(CO)_2Tcbiim]_2[Pt(CN)_2Tcbiim]$. Preliminary axial photographs indicated a monoclinic space group. Examination of the collected data yielded the following observed extinctions: $0k0$, $k = 2n + 1$. These extinctions result in ambiguous space group assignment. Two space groups exhibit the observed extinctions. These are $P2_1/m$ (No. 11) and $P2_1$ (No. 4). This ambiguity was removed by observing that in the complete solution, though the anions follow the symmetry of $P2_1/m$, the cations require $P2_1$. Crystallographic parameters appear in Table 10.S.

When the position for the cation was refined, peaks appeared in the difference map defining a noncoordinated solvent molecule. This was anticipated by the behavior of the crystals. Input of these atom positions and cycling to isotropic convergence resulted in values of $R = 5.9\%$ and $R_w = 5.8\%$.

A packing diagram clearly showed a well-defined linear metal atom stack. Analysis of individual crystals from the same group as the diffraction sample via electron microprobe yielded an iridium:platinum ratio of 2:1. The conclusion was that the isoelectronic platinum moiety was indeed substituted in the stack, producing charge compensation. Inspection of the current thermal parameters confirmed what was suggested by the microprobe analysis, that the oxygen atoms of the CO ligands of the iridium complex were disordered with the nitrogen atoms of the CN^- ligands of the platinum complex. Thermal parameters of the central metal were slightly higher than normal, but the difference between an Ir(I) and Pt(II) to an X-ray beam is negligible.

The conclusion of disorder in the CO/CN^- ligands led to calculation of anisotropic thermal parameters only for all other ligand atoms. Repeated cycling led to convergence with $R = 4.01\%$ and $R_w = 4.01\%$. In the final difference map the two largest residuals were 0.76 and 0.66 eÅ^{-3}. These were both located within 1 Å of the central metal. The final data:parameter ratio was 10.0:1, an excellent value. No evidence of any superlattice reflection was observed, either in preliminary photographs or during data collection.

Final positional and thermal parameters appear in Tables 11.S and 12.S. A plot of the asymmetric unit is shown in Figure 1.

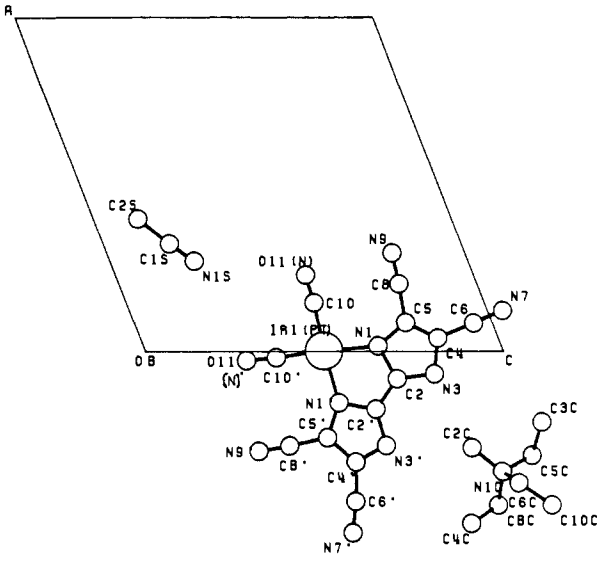

Figure 1. Asymmetric unit and atom labels for $(NEt_3Me)_3[Ir(CO_2)$-$Tcbiim]_2[Pt(CN)_2Tcbiim]$.

Results and Discussion

The Stacking Moiety: $[Ir(CO)_2Tcbiim]^-$. Several crystallographic determinations have been completed on compounds containing this coordination complex. Of these, three describe simple salts of the coordination complex. Of the crystalline forms described by single-crystal X-ray analysis, two distinct colors are observed, red and yellow. Historically, salts of Ir(I) are yellow, so it was expected that the yellow compound would yield the most undistorted view of the stacking ion.

Indeed, $NEt_3Me[Ir(CO)_2Tcbiim]$ yielded the most planar arrangement of the atoms in the molecule. This compound is yellow when crystalline, but it desolvates rapidly in air, turning red within 60 s. Redissolving and recrystallizing the red solid from CH_3CN yields the original yellow form. Figure 2 shows a view perpendicular to the stacking axis of the compound. In this view, the planarity of the molecule is clearly seen. Calculation of the least squares plane for the anion shows no atom deviating more than 0.048 Å from this plane. The central metal atom shows a deviation of only 0.0028 Å.

The N2–C3 bond on the back side of the ligand is slightly longer than the comparable N1–C4 bond on the metal side. In the free ligand these two distances[23] are virtually equal, and the same

(17) MacGillaury, C. H.; Reich, G. D.; Lonsdale, K. *The International Tables for X-ray Crystallography*; Kynock Press: Birmingham, England; VIII; 1962.
(18) Cromer, D. T.; Waber, J. T. *Acta Crystallogr.* **1965**, *18*, 104.
(19) Butler, W. M. STD-DEV; University of Michigan.
(20) GEOMIN; a crystallographic program for geometric calculation supplied by University Chemical Laboratories; Cambridge, England.
(21) Johnson, C. K. ORTEP—A Fortran Thermal Ellipsoid Plot Program for Crystal Structure Illustrations; Oak Ridge National Laboratory; 1965.
(22) PLUTO; a crystallographic plotting program supplied by University Chemical Laboratory; Cambridge, England.
(23) Anderson, James E. Ph.D. Thesis; University of Michigan, 1985.

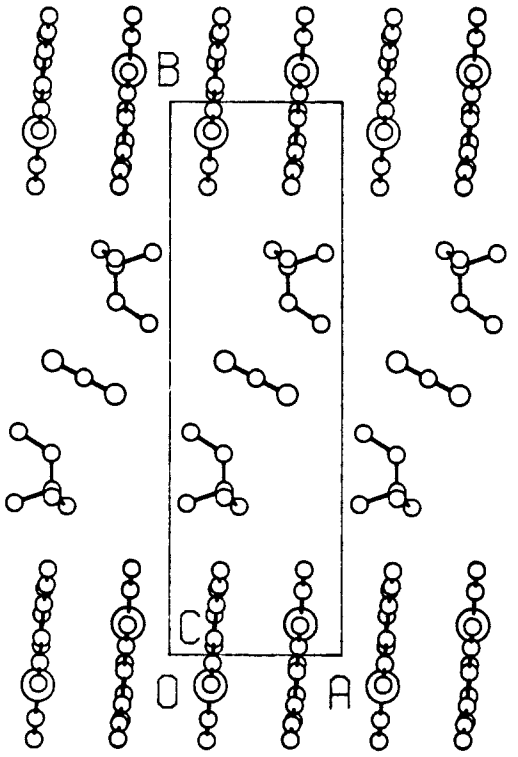

Figure 2. Stacking plot of $NEt_3Me[Ir(CO)_2Tcbiim]$.

length as the metal side N1–C2 bond. Bond lengths, shown in Table 13.S, are similar to those observed for the free ligand, except for the cyanides, which average slightly longer (0.03–0.05 Å) due to charge delocalization. The angle N1–C2–C2 on the metal side measures 113.4°, while the back side angle, N2–C2–C2, measures 130.6°. From the other ring angles in Table 14.S, this C2 center absorbs the majority of the strain.

Stacking Interactions in Unoxidized Salts of $[Ir(CO)_2Tcbiim]$. Three crystal structures have been completed on simple alkyl ammonium salts of the monoanion, $[Ir(CO)_2Tcbiim]^-$. Reported here are NEt_3Me^+ and $NEt_2Me_2^+$ (the molecular structure of $NEt_4[Ir(CO)_2Tcbiim]$ has been previously reported[24]). The dication, $NEt_2Me(CH_2)_4NEt_2Me^{2+}$, has also been synthesized and its structure with the monoanion completed. Bond lengths and angles for $NEt_2Me_2[Ir(CO)Tcbiim]$ are listed in Tables 15.S and 16.S. Tables 17.S and 18.S contain bond lengths and angles for the dication structure.

Of the four structures completed to date, three are of the red form, NEt_4^+, $NEt_2Me_2^+$, and the dication. The cation NEt_3Me^+ crystallizes in a yellow form. Stacking plots of the compounds in the monocation series appear in Figures 2, 3, and 4.

Careful comparison of these stacking diagrams shows that the NEt_3Me^+ has a completely columnar stack, with no obvious metal–metal association between the members of the stack, while the two end members of the series form discrete dimeric pairs within the stack. The compounds seen to crystallize in the dimeric pair structure are the ones that appear red in the solid state. It is the compound with no metal–metal distances under 3.6 Å that is yellow.

A similar phenomena is observable in solutions of these compounds, except that the observance of the red and yellow colors becomes independent of cation and strictly a function of temperature and concentration. In dilute solutions, all of these salts are yellow. Spectral measurements show a large band at 372 nm with a shoulder at 410 nm. These have been previously assigned to the presence of the monomeric anion $[Ir(CO)_2Tcbiim]^-$ in solution.[25] If the concentration is increased or the temperature

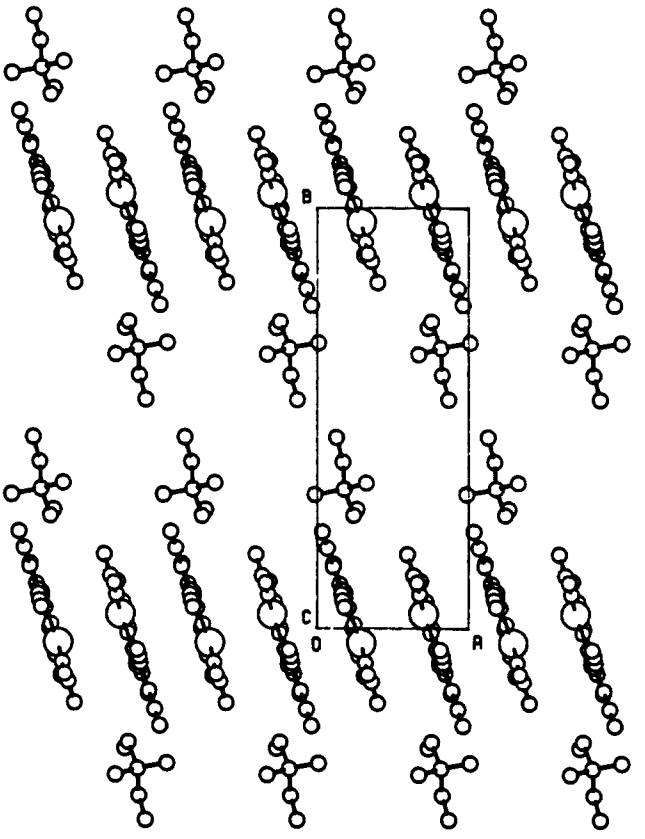

Figure 3. Stacking plot of $NEt_2Me_2[Ir(CO)_2Tcbiim]$.

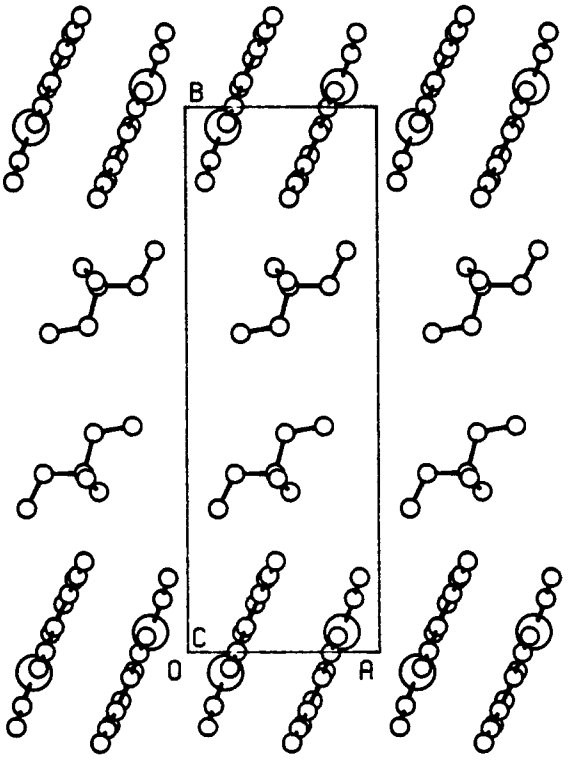

Figure 4. Stacking plot of $NEt_4[Ir(CO)_2Tcbiim]$.

reduced, the solutions darken to give a red color. Spectral measurements on the more concentrated solutions show an additional absorbance at 472 nm. This has been assigned as due to the presence of an association dimer of two monoanions in solution. The intensity of these two peaks is related. If the temperature of a red solution is raised, the intensity of the peak at 472 decreases, while the peak at 372 is seen to increase in intensity.

(24) Rasmussen, P. G.; Bailey, O. H.; Bayoñ, J. C.; Butler, W. M. *Inorg. Chem.* **1985**, *23*, 343.

(25) Tamres, M.; Bailey, O. H.; Anderson J. E.; Rasmussen, P. G. *Spectrochim. Acta* **1986**, *42A*, 741.

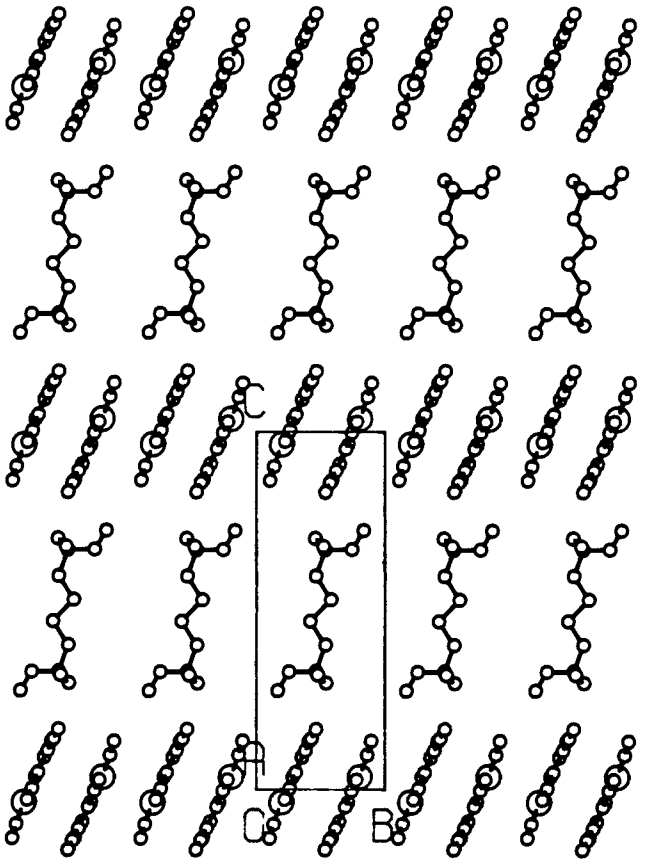

Figure 5. Stacking plot of $NEt_2Me(CH_2)_4NEt_2Me[Ir(CO)_2Tcbiim]_2$.

Table III. Metal–Metal Distances (Å) for Unoxidized Salts of $[Ir(CO)_2Tcbiim]^-$

cation	short distance	long distance	color
NEt_4^+	3.154	4.799	red
NEt_3Me^+	4.036	4.468	yellow
$NEt_2Me_2^+$	3.206	4.404	red
$NEt_2Me(CH_2)_4NEt_2Me^{2+}$	3.159	4.761	red

The dication form of the planar iridium monoanion is also identical in color with the red crystals described. It too crystallizes in an orthorhombic space group. A view of the plane containing the stacking axis is presented in Figure 5.

Inspection of this figure again reveals the presence of association dimers along the stack. These dimeric units are the likely cause of the red color of the crystal. Metal–metal distances in these compounds are presented in Table III. The distance of an iridium–iridium single bond with no bridging groups has been reported at 2.88 Å.[26] From the table, it is noted that short metal–metal distances in the red compounds are in the range of 3.2 Å.

A correlary to this observed dimer formation is noticeable distortion from planarity in the stacking anion. The van der Waals radii for this stacking unit is estimated to be ~3.46 Å when there is no apparent metal–metal interaction. The dimeric packing forces about 0.3 Å closer approach of the π clouds of the ligands than this value. The result is seen as a bending back of the ligands. In cases where dimeric pairing is observed, the iridium atom shows the greatest deviation from the least-squares plane in the direction of its partner. These deviations range from 0.08 Å in the $NEt_2Me_2^+$ case to 0.12 Å in the NEt_4^+ structure. No such distortion is observed in the structure of the yellow compound $NEt_3Me[Ir(CO)_2Tcbiim]$.

An unusual feature of the method of packing in these salts is the columnar nature of the anion packing. Figures 4.S through 7.S offer a view looking down the crystal axis parallel to the anion stack. In these views the twist angle is apparent between dimer pairs. The $NEt_2Me_2^+$ compound has a twist angle of 157° between pairs, while the twist angle in all other structures is 180°.

(26) Rasmussen, P. G.; Bailey, O. H.; Tamres, M.; Bayoñ, J. C. *J. Am. Chem. Soc.* **1985**, *107* (*1*), 280.

Table IV. Summary of Conductivity Data for $(cat)_5[Ir(CO)_2Tcbiim]_6(an)$

cat/an	ClO_4^-	BF_4^-	$PO_4Me_2^-$	HSO_4^-
$NPrEt_3^+$		m		
NEt_4^+	2×10^{-4}	7×10^{-4}		2×10^{-2}
$NPrEt_2Me^+$		4×10^{-2}		
NEt_3Me^+		2×10^{-3}		1×10^{-4}
(dication)			s	$\sim 2 \times 10^{-3}$
$NEt_2Me_2^+$		1×10^{-4}	s	
$NEtMe_3^+$		4×10^{-9}		
NMe_4^+	s	s		

Mixed-Valence Compounds of Iridium. These compounds were formed by electrochemical oxidation from the starting salts. The compounds deposited on the electrode, covering it in some cases. This covering of product did not reduce current flow and in some experiments current flow actually increased, as though the electrode area were increasing. The only conclusion is that these compounds are electrically conducting.

Analytical data on the first two members of this series of compounds, $(NEt_4)_5[Ir(CO)_2Tcbiim]_6(ClO_4)$ and $(NEt_4)_5[Ir(CO)_2Tcbiim]_6(BF_4)$, are summarized in Table 19.S. From this analysis, we formulate the oxidation state of iridium as 1.3 ± 0.2. A more accurate verification was obtained by coulometry. A measured amount of $NEt_4[Ir(CO)_2Tcbiim]$ was electrolzed under constant potential in a cell with low internal resistance. Current flow dropped to less than 5% of its initial value rather suddenly at the oxidation point Ir(1.33 ± 0.06).

Crystallographic confirmation of the anion and cation count would be the most unambiguous method of oxidation state determination if an ordered system could be found. In our attempts to grow ordered crystals on the electrode we explored a series of alkyl ammonium cations, while varying the anions incorporated with these cations. A summary of the compounds prepared and their conductivities appears in Table IV. Here the numerical values are given in terms of mhos/cm, "s" denotes a soluble product, and "m" a metastable one. In this case, metastable describes a compound that formed but decomposed before it could be removed from the cell. From this table it is clear that cations with 8 to 10 carbon atoms define the range of the better conductors. The dication is considered to be a pseudo-9-carbon cation as it has 9 carbon per unit of charge. These cations produced the only observed crystals among the mixed-valence products. Unfortunately, none of these experiments produced crystals suitable for X-ray diffraction.

As a check of the two point pellet conductivities, one case was tested with a special four-probe device described elsewhere.[9] For this experiment, the leads of the four-conductor anode were shorted outside the cell. Oxidation of $NEt_4[Ir(CO)_2Tcbiim]$ with NEt_4ClO_4 as supporting electrolyte with this shorted anode resulted in product growth across all four exposed leads of the electrode. When the shorting device was removed and the electrode taken from the cell, a conventional four-probe measurement was performed. The result was a measured conductivity of similar magnitude to that found for the two-probe conductivity.

Infrared spectra of these compounds are typical of semiconductors in that absorption edges are observed. Spectra taken of several of the better conductors are virtually identical. A very intense, broad absorption band starts outside the normal IR range (beyond 4000 cm^{-1}) and continues into the 1600-cm^{-1} region of the spectrum. This broad band is so intense it obscures any other band in this region. For the compound $(NEt_4)_5[Ir(CO)_2Tcbiim]_6(ClO_4)$, the onset of this plasma edge begins at 1900 cm^{-1}. This value corresponds to a band gap of 0.25 eV. In order to characterize the band gap more definitively, we placed a pressed pellet of this compound in an impedance bridge and measured the dielectric constant as a function of temperature at 10000 Hz. At this frequency the equivalent circuit is both resistive and

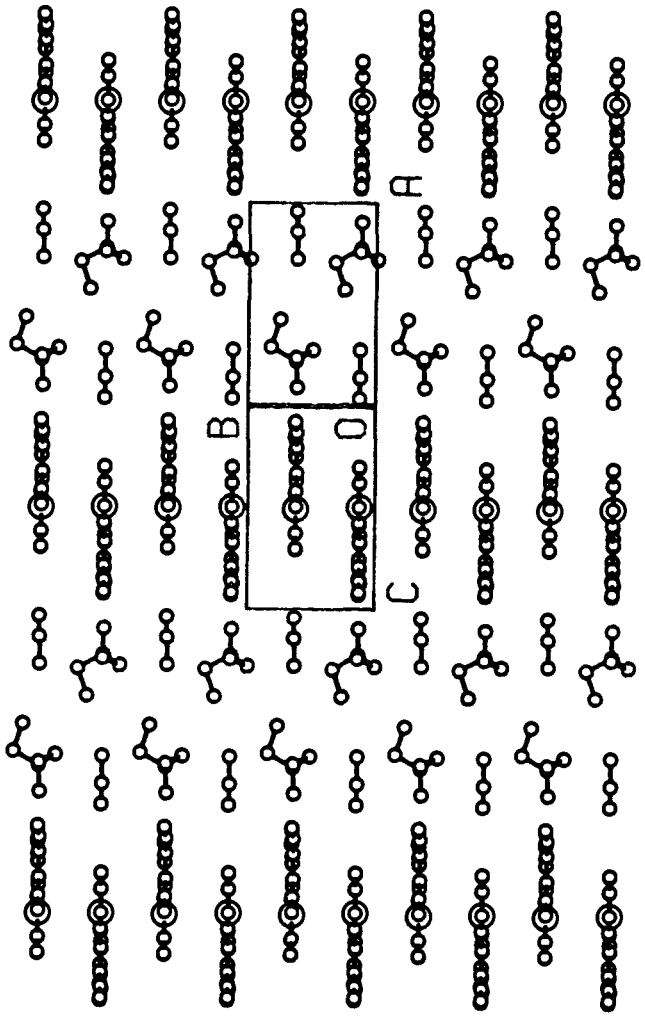

Figure 6. Stacking plot of a single plane in $(NEt_3Me)_3[Ir(CO)_2Tcbiim]_2[Pt(CN)_2Tcbiim]$.

capacitive; however, the values obtained should be proportional to bulk DC conductivity. The low-temperature limiting values; which change in linear fashion, represent the thermal coefficient of the instrument and are subtracted off by extrapolation. The resulting values give a band gap of 0.21 eV, in good agreement with that obtained from the absorption edge.

The Mixed-Valence Platinum Iridium Compound. The failure of cation and anion variation to provide ordered crystals suggested the need for a different approach to the charge compensation problem. If the soluble compound $(C(NH_2)_3)[Ir(CO)_2Tcbiim]$ is subjected to oxidation and combined with the isoelectronic analogue $(NBu_4)_2[Pt(CN)_2Tcbiim]$, a new compound, in crystalline form suitable for X-ray analysis, can be prepared.

Figure 6 describes a plane in this structure containing the anion stacks. This is the structure of a mixed-valence compound, as is evident from the linearly stacked metal atoms. In the projection plot of Figure 8.S, the metal atoms appear to be almost exactly aligned. In fact, the atoms deviate from the least-squares line containing them by less than 0.015 Å. Only one metal–metal distance is observed in the structure, and the least-squares planes containing the ligands are exactly perpendicular to the line containing the metal atoms. This metal–metal distance of 3.41 Å is longer than that for the association dimers in some unoxidized compounds, but in those cases the ligands distort away from each other in pairs which could not lead to uniform repeat distances along the stack.

The repeat distance observed here is longer than that normally found in partially oxidized complexes. It would be desirable to obtain conductivity on the Pt–Ir material, but this proved impossible due to extremely rapid desolvation. Following solvent loss, the material is noncrystalline and very fragile. Powder

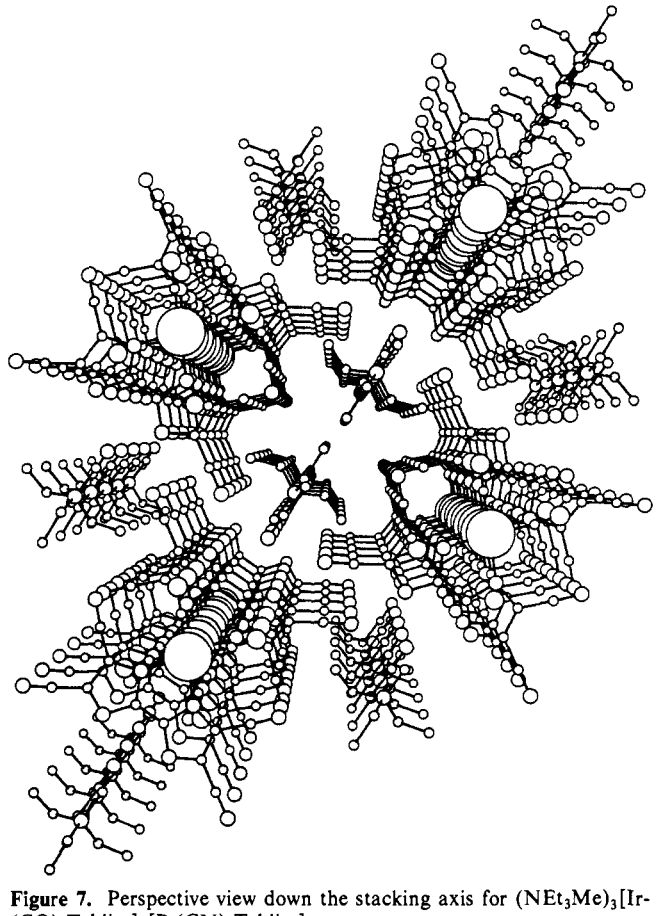

Figure 7. Perspective view down the stacking axis for $(NEt_3Me)_3[Ir(CO)_2Tcbiim]_2[Pt(CN)_2Tcbiim]$.

conductivities are normally in the range of 10^{-4} ohm^{-1} cm^{-1} (Table IV), but the metal–metal distances are unknown. It is clear that greater overlap is possible in the lower valent iridium(I) systems compared to analogous Pt(II) systems at the same distances, but from the distance observed in our mixed metal case one would predict only weak semiconducting behavior. The metal–metal distance in the amorphous iridium materials is under investigation by EXAFS and X-ray powder techniques. Preliminary work reveals more than one metal–metal distance, however, which makes correlation of the structural and physical properties difficult.

The stacking plane presented in Figure 6 is a plane parallel to the X–Z diagonal. This compound proved surprisingly easy to crystallize. Well-formed plates of 2 mm × 4 mm × 1 mm were common, and slightly larger crystals were occasionally observed. Unfortunately, the solvent seems to aid in the production of quality single crystals, but it also has the effect of making them vulnerable to atmospheric desolvation, and this occurs in 1 or 2 s once removed from a solvent-saturated atmosphere.

It is possible that this speedy desolvation is actually a function of the metal–metal attraction in the lattice. One could easily visualize a collapse along the Y axis if the solvent molecules were removed. The results of such a collapse would be closer metal–metal approach and a higher degree of interaction between the metal atoms. One further result would be a removal of the insulating layer between cations, destabilizing the lattice. Greater interaction between metal atoms is expected to produce a much darker color, and exposure to the atmosphere for more than 2 s results in transition from well-formed crystals green in cross section, to small black pieces of the former. Tables 20.S and 21.S describe bond lengths and angles for this compound.

Stacking angle is a topic that has not been addressed previously. Generally, for maximum metal d_{z^2} overlap, one would expect stacking units to be perpendicular to the metal atom chain. This has been observed for the cyanoplatinates and iridium carbonyl chlorides. The observed stacking angle in the current metal chain structure is also 0° from the perpendicular. Among the crystallized

precursers, the least deviation from this angle occurs in the unoxidized precurser $NEt_3Me[Ir(CO)_2Tcbiim]$ as 7° from the perpendicular. In the other structures, this deviation averages 30°. In this respect, the NEt_3Me^+ ion seems a particularly good choice for the charge balancing cation.

Figure 7 is a perspective plot looking down the stacking axis for the mixed-metal compound. Here the cation channel is clearly visible. Cations in this channel alternate with solvent molecules. Note the uncrowded nature of the cation channel in this structure. This observation reinforces the hypothesis that insulation between cations and resulting 'comfortable space' for the cations in the lattice contributes to the overall stability of the crystal and increases its likelihood of formation. Also visible is the apparent stacking of the nitrile nitrogens. The reason for this is not clear. As it is, the interplanar distance of 3.41 Å is not far removed from the van der Waals radius of 3.46 Å estimated from the $NEt_3Me[Ir(CO)_2Tcbiim]$ structure. It is possible that at this distance the steric interactions are unimportant. The possibility of some π-cloud interaction is also suggested. All eclipsed atoms in the complex have p orbitals participating in delocalization within the complex. Other researchers have suggested this as a possibility for iridium-containing complexes with eclipsed geometry.[27]

Summary

The main body of this work has centered on the design, preparation, and structural characterization of the family of anisotropic conductors based on the planar complex $[Ir(CO)_2Tcbiim]^-$. In the course of this work, numerous new compounds have been synthesized. The conductivity of the powder forms of the compound has been improved by several orders of magnitude, and both the soluble and insoluble forms of the compound have been characterized with respect to oxidation state.

The total number of metal ion containing anisotropic conductors is small. The partially oxidized platinum cyanides and oxalates have been reviewed by Williams.[28] The metal phthalocyanines have been reviewed by Hoffman and Ibers.[29] Conducting metal thiolate complexes have been described by Cassoux et al.[30] and by Underhill.[31] In all of these systems charge is compensated as partial oxidation occurs and various structural consequences ensue. In none of them, however, is the substitution of an isoelectronic ion employed for charge compensation.

The compound $[NEt_3Me]_3[Ir(CO)_2Tcbiim]_2[Pt(CN)_2Tcbiim]$ is unique, being the first-reported one-dimensional alloy. The possibility that the electron density centered on the metal atom is nearly uniform along the stack seems likely, given the quality of the X-ray solution for this compound.

The discovery of this metal chain system has opened many possibilities for investigation of its physical properties. Previously, iridium systems have not yielded the crystals needed to bring the level of study to those cited above. The measurement of these properties is the goal of our continuing work.

Acknowledgment. P.G.R. acknowledges support from the donors of the Petroleum Research Fund, administered by the American Chemical Society. The researchers also acknowledge the assistance of William M. Butler with the crystallographic data collection.

Supplementary Material Available: Tables 1S-21S and Figures 1S-8S giving crystallographic details and unit cell views (26 pages). Ordering information is given on any current masthead page.

(27) Krogmann, K. *Z. Anorg. Allg. Chem.* **1968**, *358*, 97.

(28) Williams, Jack *Advances in Inorganic and Radiochemistry*; Emeleus, H. J., Sharpe, A. G., Eds.; Academic Press: New York, 1983; Vol. 26, pp 235-267.

(29) Hoffman, B. M.; Ibers, J. A. *Acc. Chem. Res.* **1983**, *16*, 15-21.

(30) Bousseau, M.; Valade, L.; Legros, J. P.; Cassoux, P.; Garbauskas, M.; Interrante, L. V. *J. Am. Chem. Soc.* **1986**, *108*, 1908-1916.

(31) Ahmad, M. M.; Underhill, A. *J. Chem. Soc., Dalton Trans.* **1982**, 1065-1069.

Generation and Characterization of Highly Reactive Oxo-Transfer Intermediates and Related Species Derived from (Tetraarylporphinato)manganese(III) Complexes

Kenton R. Rodgers and Harold M. Goff*

Contribution from the Department of Chemistry, University of Iowa, Iowa City, Iowa 52242.
Received March 2, 1988

Abstract: This report presents the structural and magnetic characterization of several monomeric high-oxidation-state (porphinato)manganese complexes via low-temperature NMR and ESR spectroscopies. These complexes are generated via low-temperature reaction of (porphinato)manganese(III) complexes with OCl_2, Cl_2, or *m*-chloroperoxybenzoic acid (MCPBA). The reversible redox character of these species is demonstrated by reactions with cyclohexene or iodide ion to regenerate the respective starting materials. (Tetraphenylporphinato)manganese(III) complexes (Mn(TPP)X, where X = Cl^- or OAc^-) exhibit novel reactivity with Cl_2 and OCl_2. Reaction with OCl_2 produces an axially symmetric manganese(IV) complex **1** that is thermally converted to a manganese(III) complex with loss of axial symmetry (**2**). Reaction with OCl_2 at temperatures above -78 °C results in formation of a third and axially symmetric manganese(IV) complex **3**. This complex is also ultimately converted to **2**. Complex **2** can be cleanly generated via reaction of Mn(TPP)X with Cl_2 at low temperature. However, neither **1** nor **3** can be generated by reaction with Cl_2. The presence of 4-methylpyridine in these reaction mixtures precludes formation of **2**. Low-temperature treatment of chloro(tetramesitylporphinato)manganese(III) (Mn(TMP)Cl) with OCl_2 yields the TMP analogue of **3** (**4**). A TMP analogue of **2** cannot be produced, even by reaction with Cl_2. A complex with spectroscopic properties similar to **2** (**2a**) can be generated by electrochemical oxidation. Although **2** exhibits higher reactivity than **2a**, present evidence supports tentative assignment of both complexes as isoporphyrins. Reaction of Mn(TPP)X or Mn(TMP)Cl with OCl_2 or MCPBA in the presence of hydroxide ion yields axially symmetric manganese(IV) complexes **5** and **6**, respectively. Both of these complexes react with cyclohexene or iodide ion to regenerate the respective (porphinato)manganese(III) complex.

The past decade has been witness to a multitude of studies involving transition-metal complexes that mimic the monooxygenase activity of cytochrome P-450. While reactions of high-valent iron-containing heme models have been extensively

0002-7863/88/1510-7049$01.50/0